

## Confinement improvement triggered by the impurity injection in T-10 ECR heated plasmas

N.A.Kirneva<sup>1,2</sup>, G.M.Asadulin<sup>1</sup>, V.M.Bajkov<sup>1</sup>, A.A.Borschegovskij<sup>1</sup>, M.M.Dremin<sup>1</sup>,  
 A.Ya.Kislov<sup>1</sup>, L.A.Kluchnikov<sup>1</sup>, V.A.Krupin<sup>1</sup>, S.V.Krylov<sup>1</sup>, N.A.Mustafin<sup>1</sup>, A.R.Nemets<sup>1</sup>,  
 Yu.D.Pavlov<sup>1</sup>, I.S.Pimenov<sup>1</sup>, G.N.Ploskirev<sup>1</sup>, D.V.Ryjakov<sup>1</sup>, D.V.Sarychev<sup>1</sup>, D.S.Sergeev<sup>1</sup>,  
 N.A.Solovev<sup>1</sup>, A.V.Sushkov<sup>1</sup>, V.M.Trukhin<sup>1</sup>, E.V.Trukhina<sup>1</sup>

<sup>1</sup> National Research Center “Kurchatov Institute”, Moscow, Russia

<sup>2</sup> National Research Nuclear University MEPhI, Moscow, Russia

Impurity injection has been obtained as an attractive tool to get an improved confinement regime at high plasma density firstly in TEXTOR tokamak [1]. Then the similar effect has been observed on different tokamaks worldwide [2]. In [3] interpretation of the confinement improvement in regimes with increased edge radiation due to the impurity injection has been done basing on plasma selforganization paradigm.

Experiments focused on the investigation of the effect of the impurity puffing on plasma confinement are carried out in T-10 (limiter tokamak, major radius  $R=150$  cm, minor radius  $a=30$  cm). Usually the effect of the confinement modification is shown in T-10 by the plasma density and stored energy increase. Effect of the increase of the central electron temperature triggered by the Neon injection in T-10 was observed for the first time in discharges with ECRH/ECCD (EC current drive in co-direction to the total plasma current). Time evolution of the typical discharge is presented in Figure 1. Increase of the electron temperature, density and stored energy due to the impurity injection is clearly seen.

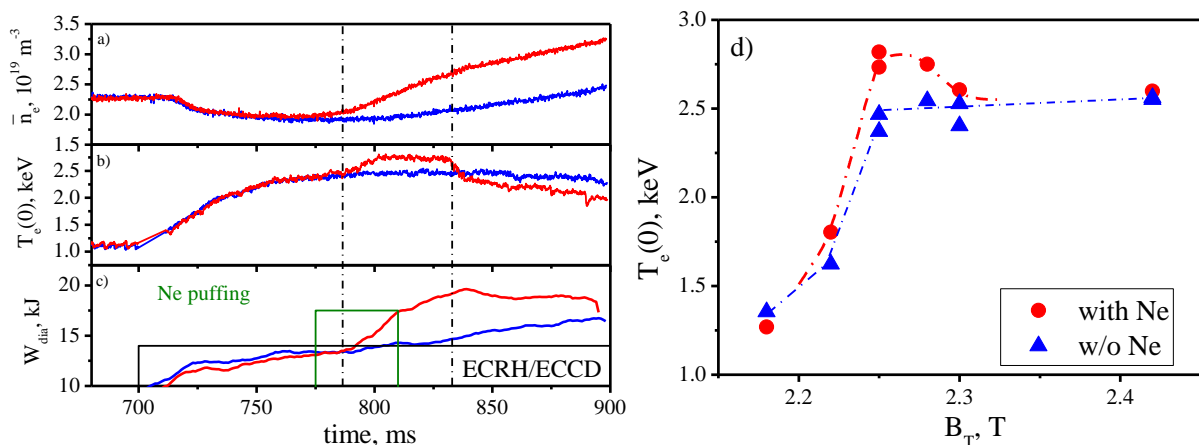


Figure 1 Traces of the plasma density (a), central electron temperature, plasma energy content (c) in two identical shots with (red curves) and without (blue curves) Neon puffing. Dependence of the central electron temperature on toroidal magnetic field in the set of similar discharges with (red points) and without (blue points) Neon puffing.

Experiments discussed here were carried out at moderate edge safety factor value  $q_{L\parallel} \sim 3$  (plasma current  $I_p \sim 240$  kA). Toroidal magnetic field was changed in the range of  $B_T = 2.42 \dots 2.18$  T, which led to the shift of the EC resonance position from the center to the high field side,  $\sim a/2$  ( $a$  - minor radius). The phenomenon of the core temperature rise appeared to be dependent on the localization of ECRH/ECCD. The highest temperature increase was observed in the regime with slightly off-axis ECRH/ECCD,  $B_T \sim 2.25$  T (Figure 1,d), when ECR power was absorbed in the vicinity of  $q=1$  position and sawtooth oscillations were suppressed. Under these conditions the Ne puffing led to the restoration of the central electron temperature up to the value observed at on-axis heating.

Increase of the radiation power caused by the Neon puffing is observed at  $r > 20$  cm (Figure 2), total radiation power increases from 0.15 (before Neon puffing) up to 0.25 (at the end of the discharge). Radiation power profiles presented in Figure 2 do not show evident signs of the impurity peaking in discharges with and without Ne puffing in spite of the sawtooth suppression. Electron temperature increases in a wide area in the plasma core (Figure 3), which confirms by the data from Thomson scattering, ECE and PHA diagnostics and by the decrease of the loop voltage. CHERS measurements show that ion temperature profiles in discharges with and without Ne puffing differ slightly and remain similar inside of the experimental error bars. Electron density profile does not peak after the impurity puffing.

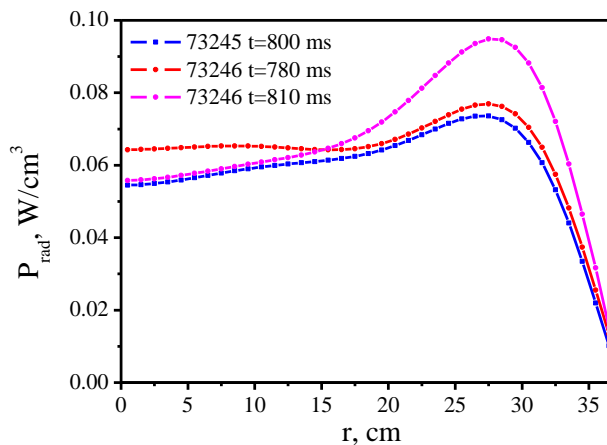


Figure 2. Radiation power profiles measured in shots with (73246) and without (73245) Ne puffing. Timing is the same as in Figure 1

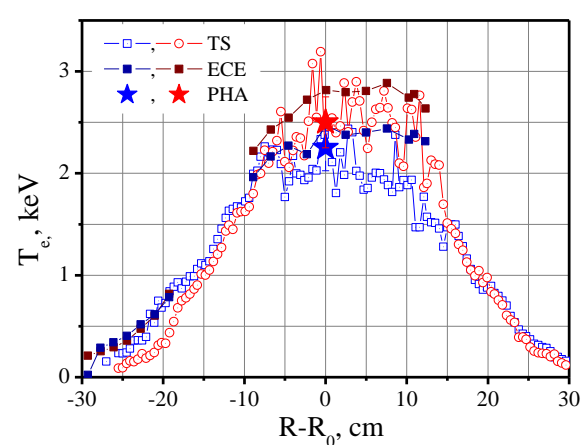


Figure 3. Electron temperature profiles measured in shots with (red points) and without (blue points) Ne puffing.

Increased core temperature regime vanishes due to the MHD mode development. The mode was identified as an odd mode, most probably  $m=1$  mode. The crash with the radius of the phase reversal  $\sim 17$  cm followed by the regular sawteeth was clearly seen by the

multichord SXR diagnostics (Figure 4). In contrast there was no sawtooth development in the same shot without Ne puffing.

Modeling of the current profile evolution was made for the discharges under investigation using the ASTRA Code [4]. Experimental evolution of the electron and ion temperature and density profiles was used. The value of the effective plasma charge was measured by the visible bremsstrahlung and CHERS at the ohmic phase of the discharge and by CHERS (Carbon) during the ECRH. The effective plasma charge was found to be close to the constant over the cross-section with  $z_{\text{eff}}=3.5$  in Ohmic and 4 during ECRH. Neoclassical conductivity was used, bootstrap current was taken into account. Electron cyclotron current profile and the value of the EC current were obtained from the OGRAY [5] calculations (Figure 5).

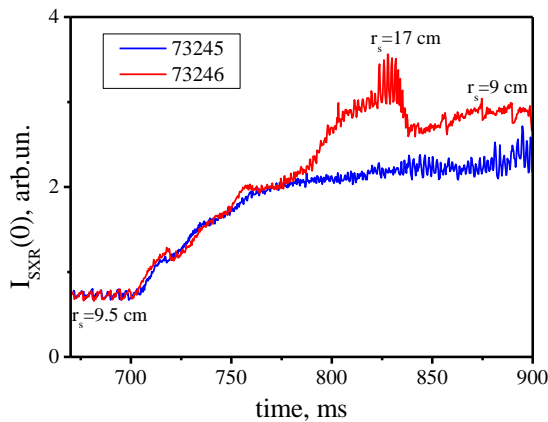


Figure 4. Comparison of the core SXR emission in shots 73246 (with Ne puffing) and 73245 (w/o Ne puffing). Inversion radius values for sawteeth and internal crash in shot 73246 ( $t=830$  ms) are presented.

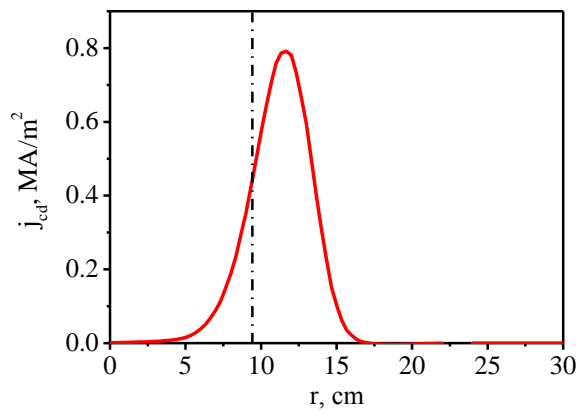


Figure 5. Electron cyclotron driven current calculated by OGRAY Code. Inversion radius of sawtooth oscillations in the ohmic phase of the discharge is shown by vertical line.

Modelled evolution of the  $q(r)$  profile is shown in Figure 6,a for the T-10 shot 73246 (with Ne puffing). ECCD leads to the formation of wide area with low magnetic shear in the vicinity of the  $q=1$  surface. Neon puffing leads to the decrease of the electron temperature on the outer third of the plasma minor radius causing a some shrinkage of the current channel (Figure 6,b). It corresponds to the experimentally observed increase of the plasma internal inductance. The shrinkage of the current channel together with the ECCD modification of the current profile lead to the further widening of the low shear area in vicinity of the  $q=1$  region. It leads to the simultaneous increase of the total heating power inside of the  $q=1$  surface.

Modeling results do not contradict to the experimental observations of MHD activity from multichannel SXR measurements. The sawtooth inversion radius during the ohmic phase obtained from the modeling is close to one observed from the SXR emission. Flattening of the

plasma current profile after co-ECCD application observed in the modeling corresponds to the sawtooth suppression observed in experiment. Broadening and then shrinkage of the  $q=1$  region do not contradict to the MHD mode  $m=1$  dynamics observed from the SXR emission and presented above.

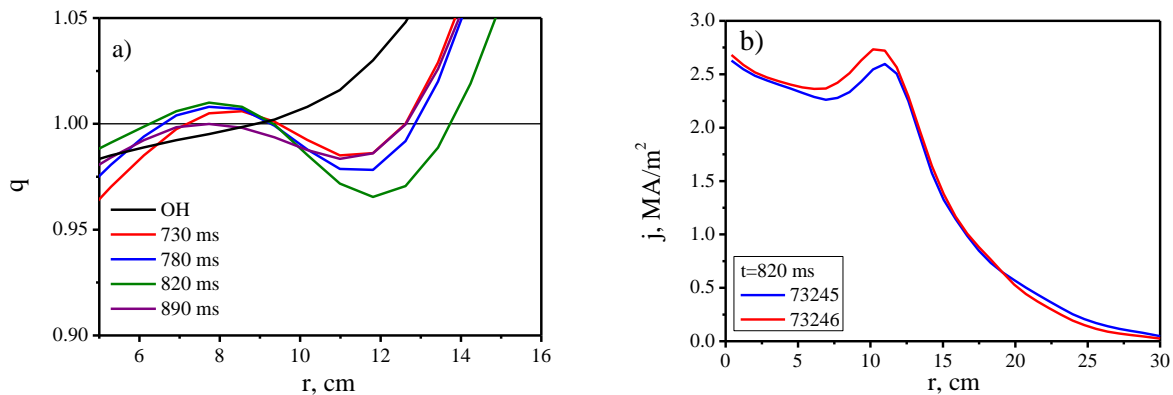


Figure 6. Modeling of the current profile evolution: a) –  $q$  profile modification in Shot 73246 with Ne puffing, b) – comparison of the plasma current profiles in discharges with (73246) and without (73245) Ne puffing.

Thus the effect of the increase of the central electron temperature after the Ne puffing in regime with slightly off-axis ECRH/ECCD appears to be the result of the confinement modification due to the  $q(r)$  evolution in vicinity of the  $q=1$  surface. Decrease of the magnetic shear and broadening of the low magnetic shear area in vicinity of the  $q=1$  region together with simultaneous increase of the heating power inside of the  $q=1$  area lead to the increase of the core temperature. Increase of the EC-current (co-ECCD) inside of the  $q=1$  surface due to the shift of the  $q=1$  position leads to the opposite effect: increase of the magnetic shear, MHD mode development and destruction of the improved confinement. This interpretation does not contradict to the features of the MHD behavior observed from SXR measurements.

This work is supported by Rosatom and by RSF (project 14-22-00193).

- [1] J. Ongena et al, in Procs. of 20<sup>th</sup> EPS Conf., Lisbon, 1993, ECA, Vol. 17C, Part I, 127
- [2] ITER Physics Basis – Nuclear Fusion, 1999, Vol.39, p.2321-2373
- [3] K.A. Razumova, Plasma Phys. Control. Fusion 60 (2018) 014037
- [4] G.V. Pereverzev, P.N. Yushmanov, ASTRA - Automated System for TRansport Analysis, IPP 5/98, February 2002
- [5] A.V. Zvonkov et al Plasma Phys. Rep. 24 (1998) 389